Full-Coverage and k-Connectivity ($k = 14, 6$) Three Dimensional Networks

Xiaole Bai*, Chuanlin Zhang†, Dong Xuan* and Weijia Jia‡
*Department of Computer Science and Engineering
The Ohio State University, Columbus, OH 43210, USA
Email: {baixia, xuan}@cse.ohio-state.edu
†Department of Mathematics
Jinan University, Guangzhou, 510632, P. R. China
Email: tclzhang@jnu.edu.cn
‡Department of Computer Science
City University of Hong Kong, Hong Kong, P. R. China
Email: wei.jia@cityu.edu.hk

***Abstract*—In this paper, we study the problem of constructing full-coverage three dimensional networks with multiple connectivity. We design a set of patterns for full coverage and two representative connectivity requirements, i.e. 14- and 6-connectivity. We prove their optimality under any ratio of the communication range over the sensing range among regular lattice deployment patterns. We also conduct a study on the proposed patterns under practical settings. To our knowledge, our work is the first one that provides deployment patterns with proven optimality that achieve both coverage and connectivity in three dimensional networks.**

I. Introduction

Three dimensional (3D) networks, particularly wireless sensor networks (WSNs), have many applications. For example, WSNs deployed in 3D aerial space can be used in supporting intelligent computer vision systems [1], helping overcome human paropsia [2], constructing aerial defense systems [3], and building aerosphere pollution monitoring systems, etc. 3D underwater WSNs also have various important applications [4] [5]. In the above applications, sensor nodes have sensing and communication capabilities, and they connect/communicate with each other to route and aggregate sensed data.

A. A Fundamental Topology Problem in 3D Networks

In this paper, we are interested in the following problem.

What is the optimal way to deploy sensor nodes in a 3D space such that the number of required nodes is minimized, the volume is fully covered, and there exist at least k disjoint paths between any two nodes?

This work was supported in part by the US National Science Foundation (NSF) CAREER Award CCF-0546668, the Army Research Office (ARO) under grant No. AMSRD-ACC-R 50521-CI; High Technology Development Program and Natural Science Foundation of Guangdong & Natural Science Foundation of P. R. China under Grant No. 2006B11201004, No. 32207013 and No. 07005930; SAR Hong Kong RGC Competitive Earmarked Research Grant (CERG) No. (CityU 114908) and CityU Applied R&D Centre (ARD(Ctr)) No. 9681001. Any opinions, findings, conclusions, and recommendations in this paper are those of the authors and do not necessarily reflect the views of the funding agencies.

This problem is fundamental in 3D WSNs. Research towards solving this problem has both theoretical and practical significance. First, minimizing the number of deployed nodes to achieve coverage and connectivity is important for economic reasons since sensor nodes deployed in 3D space are usually expensive. Second, if the optimal deployment pattern is known, it is then possible to examine the efficiency of commonly-used patterns in practical 3D deployments. Third, knowledge of optimal patterns can also provide guidance for designing topology control algorithms in 3D WSNs.

However, the above problem is hard and our knowledge of its answer is limited. There are two sets of works related to this problem that we briefly discuss here, and further discussions will be presented in Section II. One set of works is on sphere-covering problems in 3D Euclidean space in the area of discrete computational geometry. In 1887, Lord Kelvin conjectured that the deployment strategy generating Voronoi polyhedra that are 14-sided truncated octahedrons is the optimal strategy to the 3D covering problem [6]. However, until now, there has been no proof on the optimality of this strategy. Note that Kelvin's conjecture only considers coverage. Another related work by S. Alam and Z. Haas is in the area of WSNs [7]. This work considers both coverage and connectivity in 3D WSNs. It suggests a deployment pattern that creates the Voronoi tessellation of truncated octahedral cells in 3D space directly from Kelvin's conjecture, but no proof is provided on the optimality. This deployment strategy can achieve 14-connectivity when the communication range is at least $4/\sqrt{5}$ times the sensing range.

Instead of searching for 3D patterns that are optimal under all conditions, researchers have focused on studying optimal patterns under certain regularity constraints. R. Bambah in [8] first presented some results under the regularity constraints imposed by a lattice (the definition thereof will be given later). Other works follow up [9], [10], [11] and [12]. Our research on the optimal patterns in 2D space takes the similar strategy. All the patterns we proposed in [13], [14] and [15] show the

978-1-4244-3513-5/09/$25.00 ©2009 IEEE

property of regularity. Among them, some have been proved to be optimal among all possible patterns [13], and some have been proved to be optimal among all regular patterns [15].

Research interest in optimal patterns under certain regularity constraints has arisen because, besides purely theoretical intentions, many important natural constructs show strong regularity in their constructing components. In 3D space, one of the most universal and important structure with the properties of periodicity and homogeneity is the lattice. Typical examples include structures of ubiquitous crystalline solids such as coal, salt, ice, etc. In this paper, we focus on regular lattice patterns.

B. Our Contributions

As we previously mentioned, the pure 3D coverage problem has been an open problem for over 100 years. The coverage-connectivity problem in 3D WSNs is even harder. In the paper, we do not intend to solve the problem entirely; instead, we focus on solving it with respect to some regular patterns as the works in [8] [15]. We highlight our contributions of this paper as follows.

– Pattern for 14-connectivity in 3D WSNs: It is interesting to study the optimality of the pattern of 14-connectivity studied in [7]. For the first time, we prove that it is in fact optimal among regular lattice patterns for any values of the ratio of the communication range to the sensing range.

– Pattern for 6-connectivity in 3D WSNs: 14-connectivity may not always be required by some applications. Since the triangle pattern in 2D WSNs that achieves 6-connectivity is widely accepted, we focus on patterns to achieve 6-connectivity in 3D WSNs. We design a set of patterns to achieve 6-connectivity and full coverage in 3D space, and we prove that they are optimal among regular lattice patterns.

– Practical considerations: The above optimal patterns are based on the sphere-sensing and sphere-communication models. As we know, to build theoretical foundations, abstraction is inevitable. However, it is important to study the patterns under more practical models as well. In the paper, we also study our proposed patterns under practical models.

Paper Organization The remainder of this paper is organized as follows. We discuss related work in Section II. Some preliminaries are provided in Section III. In Section IV, we present our newly proposed patterns for 14- and 6-connectivity, respectively. Numerical results are also reported. In Section V, we prove the optimality of the newly proposed patterns. In Section VI, we discuss some practical considerations. Section VII concludes the paper.

II. Related Work

In this section, we classify related research into two groups. One is in the area of discrete computational geometry, and the other is in the area of wireless sensor deployment.

A. Covering and Packing in Discrete Computational Geometry

One closely-related problem in discrete computational geometry is the covering problem, especially sphere covering in 3D Euclidean space. In 1887, Lord Kelvin provided a conjectured answer to the problem of "What is the optimal way to fill a three dimensional space with cells of equal volume such that the surface area (interface area) is minimum?". This problem is equivalent to "What is the optimal way to fully cover a 3D space using the smallest number of cells?". His answer states that the Voronoi polyhedra in the optimal covering strategy are 14-sided truncated octahedrons [6]. To date, the proof for Kelvin's conjecture remains open. However, there are valuable works on the covering problem under certain conditions. One important condition is the spheres are placed following certain regularity conditions. In [8], R. Bambah first proved that the least covering density of a 3D space by identical spheres is $5\sqrt{5}\pi/24$ (the definition of covering density will be given later). This least density occurs when the sphere centers form a body-centered cubic lattice with the edges of the cube equal to $4r/\sqrt{5}$, where r is the radius of the spheres. E. Barnes in [9] and L. Few in [10] proved the same result differently. R. Bambah and other researchers later extended this result to 4D space in [11] and to n-dimensional space in [12]. None of these works considers connectivity, though they inspire us to also address the connectivity-coverage problem under regularity constraints.

Another closely-related problem is sphere packing in 3D Euclidean space. Sphere packing considers arrangements of non-overlapping identical spheres filling a space. There have been several works on the packing problem [16]. One of the most famous results is known as Kepler's conjecture. In 1611, Johannes Kepler conjectured the maximum possible density for sphere packing is $\pi/\sqrt{18}$. No rigorous proof was provided until 2005. T. C. Hales in [17] accomplished the proof showing that no packing of identical spheres in 3D Euclidean space can have a density greater than $\pi/\sqrt{18}$, which is the density of the face-centered cubic packing [17], [18], [19].

There are dozens of works on different covering problems and their variants that relate to discrete computational geometry or geometry of number. However, none of them considers both coverage and connectivity in 3D Euclidean space.

B. Connectivity and Coverage in Wireless Sensor Deployment

We studied several optimal deployment patterns to achieve multiple connectivity and full coverage in 2D WSNs in [13], [14], and [15]. The optimality of some patterns is proved under regularity constraints.

S. Alam and Z. Haas in [7] suggests the sensor deployment pattern that creates the Voronoi tessellation of truncated octahedral cells in 3D space. The suggestion follows directly from Kelvin's conjecture. By numerical comparison, [7] illustrates truncated octahedron tessellation is better than the tessellations of cubes, hexagonal prisms, and rhombic dodecahedra. However, the optimality proof for the tessellation of truncated octahedron is untouched. We note that this deployment strategy requires that the communication range must be at least $4/\sqrt{5} \approx 1.7889$ times the sensing range in order to achieve connectivity among nodes. Once this connectivity is established, the network will have at least 14-connectivity.

Besides works that focus on the optimal deployment strategy, there are some works in 3D sensor deployment that address other issues related to coverage. In [20], a deployment algorithm is proposed to "repair" coverage holes once they are discovered in a 3D volume. In [21], some sufficient conditions are presented for sensors in a given deployment to check if every point in a 3D volume is covered by at least k sensors. None of these works provides any leads towards optimal deployment patterns in 3D WSNs.

Note that there are many valuable works on 3D routing and localization, e.g., [22], [23], [24] and [25]. Our work can complement theirs by providing new network topologies in which their algorithms and protocols may be applied.

III. Preliminaries

Similar to the research on optimal deployment patterns in 2D, we assume that all sensors are the same and each has a sphere-shaped communication domain with radius r_c and a sphere-shaped sensing field with radius r_s. We also assume that the deployment region is vast enough such that its boundaries can be ignored. In Section VI, we will discuss practical considerations which are beyond these mathematical abstractions. In the following, we introduce some important definitions.

Definition 1: Right Parallelepiped, Base Diagonal, Side Diagonal, Axle Set: A hexahedron is called a right parallelepiped if its bases are parallelograms aligned one directly above the other and has lateral faces that are rectangles. The diagonals of the bases are called base diagonals. The diagonals of the lateral faces are called side diagonals. Any three edges of a parallelepiped are called an axle set if any two of them are not parallel.

Definition 2: Basic Lattice, Seed Parallelepiped: Given right parallelepiped α, set Λ is called a basic lattice generated by right parallelepiped α if Λ is composed of all the vertices generated by shifting α to its three edges' directions with shift distance being an integer times the corresponding edge length. This right parallelepiped α is called the seed parallelepiped for Λ.

For example, if α is a unit cube with edge length equal to 1, we set its one vertex as the origin point and three lines passing through the axle set intersected at this vertex as the axes of a reference frame, then the basic lattice generated by α is the set of points with integer coordinates in this reference system. In a more general case, for a given α with rectangular bases, we set one vertex of α as the origin point and three lines passing through the axle set intersected at this vertex as the axes of a reference frame, and also set the coordinate unit for each axis as the length of the edges parallelling to the axis, then the basic lattice generated by α is the set of points with integer coordinates in this reference system.

It is worth noting that one basic lattice can have different seed parallelepipeds, but it is determined as long as one of them is given.

Definition 3: Body-Centered Lattice: Given basic lattice Λ' generated by seed parallelepiped α, point set Λ is called a body-centered lattice if it is composed of all points in Λ' and all the center points of α in the process of generating Λ'.

A body-centered lattice is called body-centered cubic lattice (bcc lattice in short) when its seed parallelepiped is a cube.

In this paper, lattice Λ generated by seed parallelepiped α refers to either a basic lattice generated by α or a body-centered lattice generated by α. We use a general term *regular lattice* for such lattices.

Definition 4: Coverage Lattice with Radius r: Given lattice Λ and spheres with radius r centering at each point of Λ, Λ is called a coverage lattice with radius r if every point in the 3D volume can be covered by at least one sphere.

Definition 5: Lattice Λ Pattern: Given sensors with sensing range r_s, a sensor deployment scheme is called lattice Λ pattern if sensors are deployed at each point of coverage lattice Λ with radius r_s.

Definition 6: Covering Density: If Λ is a coverage lattice with radius r and it is generated by the seed parallelepiped α, the ratio of the total volume of the spheres with radius r that cover α to the volume of α is called covering density of Λ with radius r, denoted by $\sigma(\Lambda, r)$.

Given a fixed r_s and two lattices Λ and Λ', if $\sigma(\Lambda, r_s) < \sigma(\Lambda', r_s)$, then lattice Λ pattern is better than lattice Λ' pattern since less sensor nodes are needed in lattices Λ pattern to achieve full coverage.

Definition 7: Optimal Lattice Pattern: Given sensing range r_s, lattice Λ pattern is called the optimal lattice pattern if $\sigma(\Lambda, r_s)$ is minimum among regular lattice patterns.

The number of sensor deployment patterns in 3D WSNs is infinite. Some patterns are complicated. As we mentioned in Section II, finding and proving the optimal deployment patterns to fully cover a 3D space among all possible patterns is hard, even when connectivity is not considered. It has been noticed that many important natural constructs in 3D space show strong periodicity and homogeneity in their constructing components. One of the most universal and important structures with such properties is lattice. In this paper, we study optimal lattice patterns.

IV. Optimal Patterns

In this section, we present the optimal lattice patterns in 3D space to achieve 14- and 6-connectivity, respectively.

A. Lattice Pattern to Achieve 14-Connectivity

The lattice pattern to achieve full coverage and 14-connectivity is illustrated in Fig. 1. As shown in Fig. 1 (a1), this pattern follows a body-centered cubic (bcc) lattice generated by a cube ABCDEFGH (seed parallelepiped) and its center point O. The edge length of the cube $e = \min(4r_s/\sqrt{5}, r_c)$. We denote this bcc lattice by Λ_{14}. Sensors are deployed at each point of Λ_{14} filling the whole 3D volume.

In Fig. 1 (a1) and (a2), the solid lines represent connected links, and the dashed lines construct the cube. Due to the

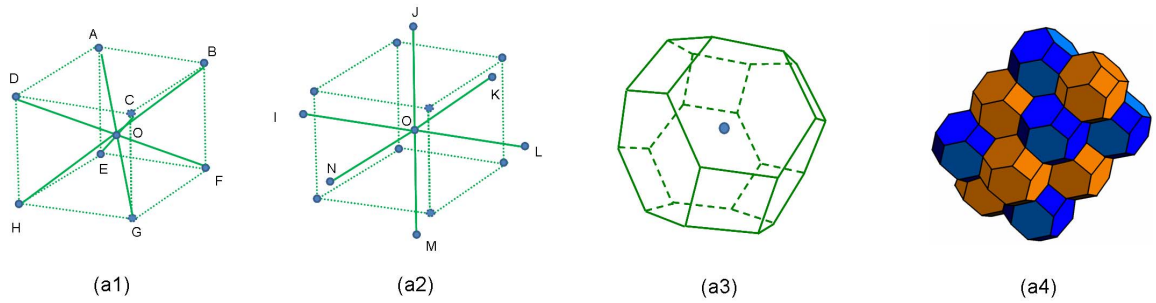

Fig. 1. Lattice pattern to achieve full coverage and 14-connectivity. Solid circular dots denote sensors. In (a1) and (a2), the solid lines represent connected links and the dashed lines construct a cube (seed parallelepiped). Consider the sensor at O, eight of its 14 connected neighboring sensors are at the vertices of the cube, and its another six neighbors are at the centers of six neighboring cubes. (a3) The Voronoi polyhedron generated by each sensing sphere is a truncated octahedron. (a4) The lattice pattern achieves full coverage of a 3D volume, which is illustrated by Voronoi polyhedra generated by sensing spheres.

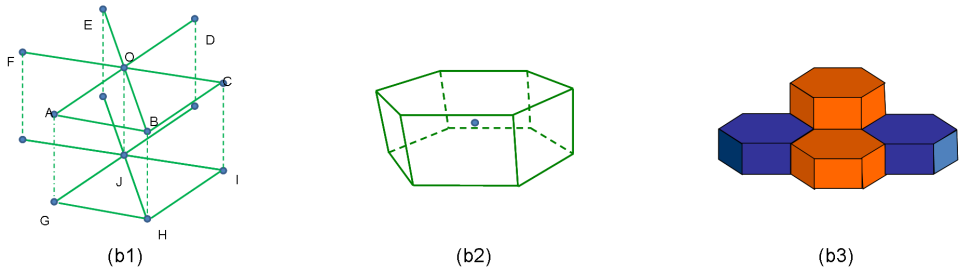

Fig. 2. Lattice patterns to achieve full coverage and 6-connectivity. Solid circular dots denote sensors. When $r_c/r_s < 9/\sqrt{43}$, the pattern is shown in (b1), (b2) and (b3). In (b1), the solid lines represent connected links. The seed parallelepiped is ABCOGHIJ. (b2) illustrates the Voronoi polyhedron generated by one sensing spheres in this pattern. (b3) shows that this pattern achieves full coverage of a 3D volume, which is illustrated by Voronoi polyhedra generated by sensing spheres. When $9/\sqrt{43} \leq r_c/r_s < 2\sqrt{3}/\sqrt{5}$, the pattern is a bcc lattice similar to that shown in Fig. 1 (a1) with edge length $2r_c/\sqrt{3}$. When $2\sqrt{3}/\sqrt{5} \leq r_c/r_s$, the pattern is also similar to that shown in Fig. 1 (a1) but with edge length $4r_s/\sqrt{5}$.

property of symmetry, each point in Λ_{14} can be considered the center of a cube when the boundaries of the 3D volume are ignored. Without loss of generality, we use the sensor at position O to illustrate connectivity. Eight of its 14 connected neighboring sensors are at the vertices of the cube (sensors at position A, B, C, D, E, F, G, and H) and another six are at the centers of this cube's six neighboring cubes (sensors at position I, J, K, L, M and N). As shown in Fig. 1 (a3), the Voronoi polyhedron generated by each sensing sphere in such pattern is a truncated octahedron. Fig. 1 (a4) illustrates that the full coverage of a 3D volume is achieved by showing relative positions of Voronoi polyhedra generated by sensing spheres.

Theorem 1: Lattice Λ_{14} pattern is an optimal lattice pattern to achieve full coverage and 14-connectivity in 3D space.

B. Lattice Pattern to Achieve 6-Connectivity

For different ranges of r_c/r_s, the lattice patterns to achieve full coverage and 6-connectivity in 3D space are different.

– When $r_c/r_s < 9/\sqrt{43}$, the pattern is a basic lattice, denoted by Λ_{6-1}, which is generated by seed parallelepiped α with diamond-shaped bases with edge length $e_1 = r_c$ and one base diagonal equal to e_1. The height of α is $h = 2\sqrt{(2r_c r_s^2 + r_s^3 - r_c^3)/(2r_c + r_s)}$. This seed parallelepiped α is illustrated by ABCOGHIJ in Fig. 2 (b1). Consider a sensor at position O. Its six neighbors (sensors at position A, B, C, D, E, and F) are all in the same plane ABCO resides on. Note that sensor nodes are connected into layers in this pattern. To ensure the global connectivity, every two layers should be connected by adding some sensors. Fig. 2 (b2) shows that in this lattice pattern the Voronoi polyhedron generated by each sensing sphere is a hexagonal prism. Fig. 2 (b3) illustrates 3D space filling of Voronoi polyhedra generated by sensing spheres centering at each point of Λ_{6-1}. Clearly, full coverage is achieved.

– When $9/\sqrt{43} \leq r_c/r_s < 2\sqrt{3}/\sqrt{5}$, the pattern is a bcc lattice generated by a cube with edge length $e_2 = 2r_c/\sqrt{3}$. This lattice is denoted by Λ_{6-2}. The cube is similar to the one illustrated by ABCDEFGH in Fig. 1 (a1).

– When $2\sqrt{3}/\sqrt{5} \leq r_c/r_s$, the lattice pattern is a bcc lattice generated by a cube which is also similar to the cube ABCDEFGH in Fig. 1 (a1). The difference is the edge length of the seed cube here is $e_3 = 4r_s/\sqrt{5}$. This bcc lattice generated by such a cube is denoted by Λ_{6-3}.

We notice that, when $9/\sqrt{43} \leq r_c/r_s < 2\sqrt{3}/\sqrt{5}$, the lattice Λ_{6-2} pattern actually achieves 8-connectivity. As shown in Fig. 1 (a1), the sensor at position O has eight connected neighbors that are at the vertices of the cube (sensors at position A, B, C, D, E, F, G, and H). When $2\sqrt{3}/\sqrt{5} \leq r_c/r_s < 4/\sqrt{5}$, Λ_{6-3} also achieves 8-connectivity. When $4/\sqrt{5} \leq r_c/r_s$, the lattice Λ_{6-3} pattern achieves 14-connectivity. As shown in Fig. 1 (a2), the sensor at position O has another six connected neighbors that are at the centers of the cube's six neighboring cubes (sensors at position I, J,

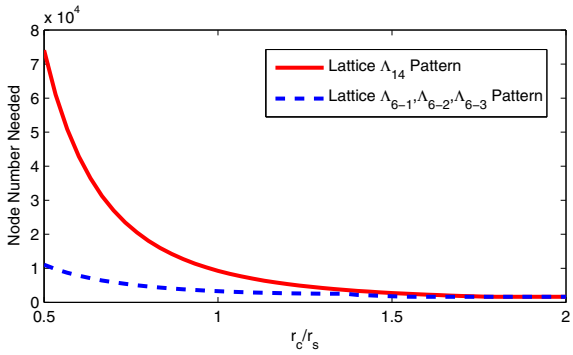

Fig. 3. The numbers of sensor that are needed for various r_c/r_s to achieve 14- and 6-connectivity by optimal lattice patterns, respectively. The 3D deployment space is $1,000^3\text{m}^3$. Sensing range r_s is 30m and communication range r_c varies from 15m to 60m.

K, L, M and N).

Theorem 2: To achieve full coverage and 6-connectivity in 3D space, the lattice Λ_{6-1} pattern is an optimal lattice pattern when $r_c/r_s < 9/\sqrt{43}$, the lattice Λ_{6-2} pattern is an optimal lattice pattern when $9/\sqrt{43} \leq r_c/r_s < 2\sqrt{3}/\sqrt{5}$, the lattice Λ_{6-3} pattern is an optimal lattice pattern when $2\sqrt{3}/\sqrt{5} \leq r_c/r_s$.

C. Numerical Results

We show in Fig. 3 the numbers of sensor node that are needed to achieve 14- and 6-connectivity respectively by optimal lattice patterns for various r_c/r_s. The sensing range r_s is 30m. The communication range r_c varies from 15m to 60m. Sensors are deployed in a 3D space with volume $1,000^3\text{m}^3$. From Fig. 3, when $r_c/r_s = 0.5$, the number needed to achieve 14-connectivity is around 6 times that to achieve 6-connectivity. This difference decreases as r_c/r_s increases. When $r_c/r_s = 1$, the number needed to achieve 14-connectivity is around 3 times that to achieve 6-connectivity. When $r_c/r_s = 4/\sqrt{5}$, the lattice patterns to achieve 14-connectivity and 6-connectivity converge such that the number needed to achieve 14-connectivity is the same as that to achieve 6-connectivity when $4/\sqrt{5} \leq r_c/r_s$.

V. Pattern Optimality

In this section, we study optimality of the proposed lattice patterns. We first present the methodology and then the proofs.

A. Methodology

Our methodology of proving the optimality of lattice Λ_{14} pattern and lattice $\Lambda_{6-1}, \Lambda_{6-2}$ and Λ_{6-3} patterns consists of two major steps.

The first step is to shrink working space that contains numerous regular lattice patterns with desirable connectivity and full coverage into a smaller set. At the second step, for each case in the set generated at the first step, we convert the corresponding minimal covering density problem to a constrained nonlinear optimization problem, and then solve it. During the conversion, all coverage and connectivity constraints are considered explicitly. After having obtained the minimal covering density value for each case, we make comparison of them to find the least one among all cases. The patterns that can generate the least value of covering density are optimal among all regular lattice patterns.

B. Optimality Proof

In this section, we present the proof for the optimality of the lattice Λ_{14} pattern stated in Theorem 1. The proof for Theorem 2, which is based on the same methodology and techniques, is briefed in Appendix. Some proof details are skipped in this paper due to the space limitations.

Step 1: We start our proof from listing all the possible cases that can achieve 14-connectivity. Surrounding a lattice vertex, there are two axle sets that can provide at most six connectivity links. Since a lattice is generated by a seed parallelepiped, there are eight congruent seed parallelepipeds surrounding each lattice point. Hence, there are at most eight body diagonals that can serve as the connectivity link for each lattice point. Also each lattice point is the intersection point generated by three planes on which there are four faces each from one surrounding parallelepipeds. These four faces that are in the same plane are congruent parallelograms surrounding this lattice point. Hence, there are at most 12 face diagonals that can serve as connectivity links for each lattice point, among which there are eight side diagonals and four base diagonals.

We shrink the number of cases as follows. First, we use the properties of a parallelogram and a right parallelepiped. One parallelogram has two diagonals. At least one of them must not be shorter than the four parallelogram edges. If both diagonals of a parallelogram are connectivity links, then its edges must be also connectivity links. One right parallelepiped has two pairs of body diagonals. And at least one pair of them must not be shorter than all the parallelepiped edges. If four body diagonals in a parallelepiped are all connectivity links, then all the edges of this parallelepiped must be also connectivity links. Second, we use the symmetry property of a lattice. In lattice patterns, connectivity links always appear in pairs. In basic lattices, the body diagonals of one seed parallelepiped can be considered as the side diagonals of another type of seed parallelepiped. Similarly, in basic lattices the base diagonals of one seed parallelepiped can also be considered as the edge of another type of seed parallelepiped. Third, if two cases are considered and case one can imply case two, we only need to consider the latter one. This is because the constraints at case two are more relaxed.

We finally need to consider one case for basic lattice patterns and eight cases for body-centered lattice patterns to achieve 14-connectivity. These cases are presented as follows.

– For each lattice point at basic lattice patterns, the connected links are:

Case A: Two axle sets and eight side diagonals. These eight side diagonals are in two planes each with four.

– For each lattice point at body-centered lattice patterns, the connected links are:

Case A: Four edges in a plane going through lateral faces, four side diagonals in a plane, two base diagonals and four body diagonals in a plane.

Case B: Four edges in a plane going through the base, four base diagonals, and six body diagonals.

Case C: Two axle sets and eight body diagonals.

Case D: Four edges in a plane going through lateral faces, four base diagonals, and six body diagonals.

Case E: Two axle sets, four side diagonals in a plane, and four body diagonals in a plane.

Case F: Four edges and four side diagonals in one plane going through lateral faces, two base diagonals, and four body diagonals in a plane.

Case G: Two axle sets and eight side diagonals.

Case H: Two axle sets, four side diagonals in a plane, and four base diagonals.

Step 2: For each case in both basic lattice patterns and body-centered lattice patterns that can achieve 14-connectivity, we are to obtain the maximum volume of the seed parallelepiped, which is denoted by V_{MAX}, such that the corresponding covering density reaches the minimum, which is denoted by $\sigma(\Lambda, r_s)_{MIN}$ (σ_{MIN} in short).

We begin with *Case A* of the basic lattice pattern. In a seed parallelepiped, denote the lengths of two edges in the base by x and y, the angle between them by γ, and the height by z. The coverage and connectivity requirements can be transformed to several inequalities of variables (x, y, z and γ). And the problem on maximal volume V'_{MAX} of the seed parallelepiped is then a constrained nonlinear optimization problem as follows.

$$\max \ f(x,y,z,\gamma) = xyz\sin\gamma, \tag{1}$$

$$s.t. \begin{cases} x^2+y^2-2xy\cos\gamma+z^2\sin^2\gamma \le 4r_s^2\sin^2\gamma \\ x^2+z^2 \le r_c^2 \\ y^2+z^2 \le r_c^2 \\ x \le r_c,\ y \le r_c,\ z \le r_c \end{cases}. \tag{2}$$

In (2), the first inequality reflects the requirement on coverage, and others are from the requirement on connectivity.

We obtain the solution of the above optimization problem as follows.

– When $r_c/r_s < 2\sqrt{3}/\sqrt{5}$, $x = y = \sqrt{2}r_c/\sqrt{3}$, $z = r_c/\sqrt{3}$ and $\gamma = \pi/2$, the seed parallelepiped takes maximal volume $V'_{MAX-1} = 2r_c^3/3\sqrt{3}$ and the corresponding converge density $\sigma'_{MIN-1} = 2\sqrt{3}\pi r_s^3/r_c^3$.

– When $2\sqrt{3}/\sqrt{5} \le r_c/r_s < \sqrt{10}/\sqrt{3}$, we obtain the solution as follows. When $x = y = \sqrt{(4r_s^2-r_c^2)(1+a)/(1-a)}$, $z = \sqrt{(2r_c^2-4r_s^2-4ar_s^2)/(1-a)}$, and $\gamma = \arccos a$, the seed parallelepiped takes maximal volume $V'_{MAX-1} = (4r_s^2-r_c^2)(1+a)\sqrt{2(1+a)(r_c^2-2r_s^2-2ar_s^2)}$ and the corresponding converge density $\sigma'_{MIN-1} = 4\pi r_s^3/[3(4r_s^2-r_c^2)(1+a)\sqrt{2(1+a)(r_c^2-2r_s^2-2ar_s^2)}]$, where $a = (r_c^2+8r_s^2-\sqrt{r_c^4-64r_c^2r_s^2+256r_s^4})/(8r_s^2)$.

– When $\sqrt{10}/\sqrt{3} \le r_c/r_s$, $x = y = \sqrt{2}r_s$, $z = 2r_s/\sqrt{3}$ and $\gamma = \pi/3$, the seed parallelepiped takes maximal volume $V'_{MAX-1} = 2r_s^3$ and the corresponding converge density $\sigma'_{MIN-1} = 2\pi/3$.

We then consider the scenarios where the deployment pattern is a body-centered lattice.

We consider *Case C*, *Case E*, *Case G* and *Case H* first. The connectivity links in these four cases all contain two axle sets. The upper bound of maximal volume V'_{MAX-u} of the seed parallelepiped for these four cases can be formulated as a constrained nonlinear optimization problem as follows.

$$\max \ f(x,y,z,\gamma) = xyz\sin\gamma, \quad s.t. \tag{3}$$

$$\begin{cases} z^2+y^2-x^2-2y\sqrt{4r_s^2-x^2}\sin\gamma \le 0 \\ z^2+x^2-y^2-2x\sqrt{4r_s^2-y^2}\sin\gamma \le 0 \\ x+y\cos\gamma-\sqrt{4r^2-z^2}-\sqrt{4r_s^2-y^2\sin^2\gamma} \le 0 \\ y+x\cos\gamma-\sqrt{4r^2-z^2}-\sqrt{4r_s^2-x^2\sin^2\gamma} \le 0 \\ y^2+z^2-x^2-2z\sqrt{4r_s^2-x^2} \le 0 \\ x^2+z^2-y^2-2z\sqrt{4r_s^2-y^2} \le 0 \\ x \le 2r_s,\ y \le 2r_s \\ 0 < \gamma \le \pi/2 \\ x \le r_c,\ y \le r_c,\ z \le r_c \end{cases}. \tag{4}$$

In (4), the first eight inequalities are from the requirement on coverage, and the others are from the requirement on connectivity. We then obtain the solution as follows.

– When $r_c/r_s < 4/\sqrt{5}$, $x = y = z = r_c$ and $\gamma = \pi/2$, the seed parallelepiped takes maximal volume $V'_{MAX-u} = r_c^3$ and the corresponding lower bound of converge density $\sigma'_{MIN-\ell} = 8\pi r_s^3/(3r_c^3)$.

– When $4/\sqrt{5} \le r_c/r_s$, $x = y = z = 4r_s/\sqrt{5}$ and $\gamma = \pi/2$, the seed parallelepiped takes maximal volume $V'_{MAX-u} = 64r_s^3/(5\sqrt{5})$ and the corresponding lower bound of converge density $\sigma'_{MIN-\ell} = 5\sqrt{5}\pi/24$.

Similarly, we can obtain V'_{MAX}'s and σ'_{MIN}'s for *Case A*, *Case B*, *Case D* and *Case F* in the body-centered lattice deployment pattern by only changing the constraints from connectivity requirement in the nonlinear optimization problem. Note that above $\sigma'_{MIN-\ell}$ is achieved at *Case C*. All the results are presented in Fig. 4.

We are now ready to get the optimal lattice pattern with the smallest covering density σ_{MIN} by comparing all σ'_{MIN}'s in in Fig. 4. We have $\sigma_{MIN} = 8\pi r_s^3/(3r_c^3)$ when $r_c/r_s < 4/\sqrt{5}$ and $\sigma_{MIN} = 5\sqrt{5}\pi/24$ when $4/\sqrt{5} \le r_c/r_s$. This concludes the proof for Theorem 1.

Please refer to Appendix for the proof of Theorem 2, which follows the same methodology and technique.

VI. Practical Setting Considerations

In this section, we discuss some practical issues beyond our mathematical abstraction.

On Practical Sensing and Communication Models: In underwater networks, there is no well accepted model for sensing

Basic Lattice	Case A	$r_c/r_s < 2\sqrt{3}/\sqrt{5}: \ \sigma'_{MIN} = \frac{2\sqrt{3}\pi r_s^3}{r_c^3}$; $r_c/r_s \geq \sqrt{10}/\sqrt{3}: \ \sigma'_{MIN} = \frac{2\pi}{3}$. $2\sqrt{3}/\sqrt{5} \leq r_c/r_s < \sqrt{10}/\sqrt{3}: \sigma'_{MIN} = \frac{4\pi r_s^3}{3(4r_s^2 - r_c^2)(1+a)\sqrt{2(1+a)(r_c^2 - 2r_s^2 - 2ar_s^2)}}$; $a = (r_c^2 + 8r_s^2 - \sqrt{r_c^4 - 64r_c^2 r_s^2 + 256r_s^4})/(8r_s^2)$
Body Centered Lattice	Case A	$r_c/r_s < 4/\sqrt{5}: \ \sigma'_{MIN} = 16\sqrt{2}\pi r_s^3/(3r_c^3)$; $r_c/r_s \geq 4/\sqrt{5}: \ \sigma'_{MIN} = 5\sqrt{5}\pi/3$.
	Case B	$r_c/r_s < 2\sqrt{2}/\sqrt{11}: \ \sigma'_{MIN} = 16\pi r_s^3/(3\sqrt{3}r_c^3)$; $r_c/r_s \geq 2\sqrt{2}/\sqrt{11}: \sigma'_{MIN} = 16\pi r_s^3/(3r_c^2\sqrt[4]{8r_c^2r_s^2 - 4r_c^4})$.
	Case C	$r_c/r_s < 4/\sqrt{5}: \ \sigma'_{MIN} = 8\pi r_s^3/(3r_c^3)$; $r_c/r_s \geq 4/\sqrt{5}: \ \sigma'_{MIN} = 5\sqrt{5}\pi/24$.
	Case D	$r_c/r_s < 4/\sqrt{5}: \ \sigma'_{MIN} = 16\pi r_s^3/(3r_c^3)$; $r_c/r_s \geq 4/\sqrt{5}: \ \sigma'_{MIN} = 10\sqrt{2}\pi/3$.
	Case E	$r_c/r_s < 4/\sqrt{5}: \ \sigma'_{MIN-\ell} = 8\pi r_s^3/(3r_c^3)$; $r_c/r_s \geq 4/\sqrt{5}: \ \sigma'_{MIN-\ell} = 5\sqrt{5}\pi/24$.
	Case F	$r_c/r_s < 4\sqrt{2}/\sqrt{5}: \ \sigma'_{MIN} = 16\sqrt{2}\pi r_s^3/(3r_c^3)$; $r_c/r_s \geq 4\sqrt{2}/\sqrt{5}: \ \sigma'_{MIN} = 5\sqrt{5}\pi/24$.
	Case G	$r_c/r_s < 4/\sqrt{5}: \ \sigma'_{MIN-\ell} = 8\pi r_s^3/(3r_c^3)$; $r_c/r_s \geq 4/\sqrt{5}: \ \sigma'_{MIN-\ell} = 5\sqrt{5}\pi/24$.
	Case H	$r_c/r_s < 4/\sqrt{5}: \ \sigma'_{MIN-\ell} = 8\pi r_s^3/(3r_c^3)$; $r_c/r_s \geq 4/\sqrt{5}: \ \sigma'_{MIN-\ell} = 5\sqrt{5}\pi/24$.
Optimal		$r_c/r_s < 4/\sqrt{5}: \ \sigma_{MIN} = 8\pi r_s^3/(3r_c^3)$; $r_c/r_s \geq 4/\sqrt{5}: \ \sigma_{MIN} = 5\sqrt{5}\pi/24$.

Fig. 4. Comprehensive results of three cases for both basic lattice patterns and body-centered lattice patterns to achieve full coverage and 14-connectivity. σ'_{MIN} denotes the minimum covering density of each case. $\sigma'_{MIN-\ell}$ denotes the lower bound of the minimum covering density. σ_{MIN} denotes the minimal covering density among all cases.

or communication along every possible 3D direction. In this paper, we consider practical models in the aerial space.

S. Megerian *et al.* in [26] propose that the quality of sensing gradually attenuates with increasing distance. Y. Zhou *et al.* in [27] propose a probabilistic sensing model where the detection probability changes for different target distance. When the above models are used, sensing sphere can still be obtained by setting a sensing range threshold that is decided by desirable sensing quality or detection probability. For some sensor types, the sensing capability may vary along different directions. One typical model obtained from real device experiments by Cao *et al.* in [28] suggests the sensing capability roughly follows Gaussian distribution over different directions. Denote the average sensing radius over all the directions by μ and the standard deviation by σ^2. In a particular direction, the probability for sensing range X being x is given by $P\{X = x\} = e^{-\frac{(x-\mu)^2}{2\sigma^2}}/(\sigma\sqrt{2\pi})$. As σ increases, the sensing field is more close to a sphere. We study by simulation the impact from such sensing irregularity on coverage in lattice Λ_{14} pattern. The results are shown in Fig. 5. We notice that higher sensing irregularity will result in lower overall coverage when other parameters are given. We also observe that, smaller r_c can help overcome the coverage shrinking contributed by sensing irregularity. This can be explained from the view of overlapped area. Smaller r_c will generate more overlapped area such that the deployment are more tolerant to sensing irregularity. When $4/\sqrt{5} \leq r_c/r_s$, the coverage will not change since the deployment pattern keeps same.

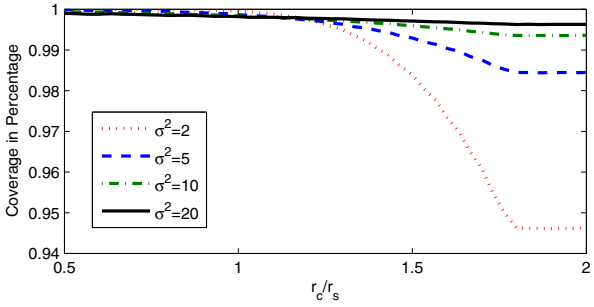

Fig. 5. Sensors each with $\mu = 30m$ are deployed in a $1000^3 m^3$ cube following the lattice Λ_{14} pattern. The coverage in percentage is obtained by first generating $1,000,000$ points within the cube, and then checking how many percent of them are covered. Every value presented is the average over 500 times simulation.

The simulation results for 6-connectivity pattern generate the same observation. We do not present them due to the space limitations.

In reality, the communication wireless signal undergoes attenuation and various disruptive physical phenomena in the air. We consider a widely used model suggested by Zuniga and Krishnamachari in [29]. This model established the function of the distance between the transmitter and the receiver and the communication link quality measured by packet reception rate (PRR). PRR at distance d can be expressed as $PRR(d) = (1 - \frac{1}{2}e^{-\frac{P_t - PL(d) - P_n}{2}})^{8\ell}$, where P_t is the output power of the transmitter, $PL(d)$ is the path loss at distance d, P_n is the

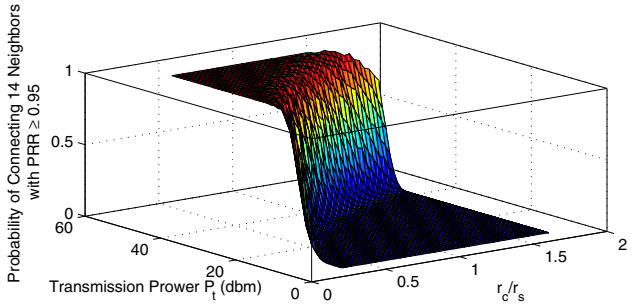

Fig. 6. A connection is considered established when $PRR \geq 0.95$. $r_c/r_s = 0.3 \sim 1.8$. For each combination of P_t and an optimal deployment pattern, we run simulation $10,000$ times. The probability is then the ratio of number of times over $10,000$ when a sensor can connect with 14 neighbors. Other parameters are from empirical data [29].

noise floor and ℓ is the frame length. (Interested reader may refer to [29] for detailed derivation.) Under this model, we consider a connection established between two nodes only if the PRR from each other is above a certain threshold. By simulation, we investigate the effect from the above model on the probability for one sensor in lattice Λ_{14} pattern to connect all 14 neighbors. The results are shown in Fig. 6. (The results for 6-connectivity lattice pattern are similar and not presented here due to the limitations of space.) We notice from Fig. 6 that that probability transition from 1 to 0 is sharp. This implies the connectivity will deteriorate fast when transmission power decreases in lattice Λ_{14} pattern.

On deployment error: Individual sensors sometimes will not be exactly deployed at the precalculated locations due to deployment errors. Denote the maximum random error by ε. In a conservative way, to ensure coverage and connectivity, we can use $r_s' = r_s - \varepsilon$, and $r_c' = r_c - \varepsilon$ to decide sensing and communication sphere and then optimal patterns accordingly.

On geographical constraints in sensor deployment: In practice, the sensor deployment space is bounded and there can exist some locations where deployment is infeasible. If all these are considered in exploring optimal deployment patterns, there are numerous specific scenarios and the results are specific. The optimal deployment patterns we proposed can act as valuable references to guide real-world deployment to avoid ad-hoc deployments in 3D spaces, especially when the deployment space is large.

On heterogeneity of sensor nodes: Nodes in 3D spaces may not be homogenous. There can be certain powerful gateways. In such cases, our optimal patterns are still valuable. In a simple example, we can consider the sensor to gateway communication range as r_s, and the gateway to gateway communication range as r_c. Ensuring that the whole network is fully covered (with coverage range r_s) as well as multiple-connected (with communication range r_c) means that each sensor in the network can communicate directly with at least one gateway and each gateway has multiple routing paths to other gateways.

VII. Conclusion

In this paper, we studied the problem of constructing connected and full covered optimal 3D WSNs. We designed a set of patterns for 14- and 6- connectivity and full coverage, and proved their optimality under any values of r_c/r_s, among regular lattice patterns. It is the first step towards providing deployment patterns with proved optimality for 3D WSNs. One of our future work is to explore other connectivity patterns. We will also study the impact on these optimal patterns from sophisticated practical settings, e.g., when flow or drift models in air or water are considered.

References

[1] M. Campbell, "Intelligence in three dimensions: we live in a 3-d world, and so should computers," *http://www.neptec.com/News2006/1Oct06-MilAero.html*, 2006.
[2] M. K. Watfa, "Practical applications and connectivity: Algorithms in future wireless sensor networks," *International Journal of Information Technolog*, vol. 4, pp. 18–28, 2007.
[3] "Aerial common sensor (acs)," *http://www.globalsecurity.org/intell/ systems/acs.htm*, 2007.
[4] J. Partan, J. Kurose, and B. N. Levine, "A survey of practical issues in underwater networks," *WUWNet*, 2006.
[5] J. Heidemann, W. Ye, J. Wills, A. Syed, and Y. Li, "Research challenges and applications for underwater sensor networking," *IEEE Wireless Communications and Networking Conference*, 2006.
[6] Thomson and S. W. (Lord Kelvin), "On the division of space with minimum partition area," *Philosophical Magazine*, no. 24, pp. 503–514, 1887.
[7] S. M. N. Alam and Z. J. Haas, "Coverage and connectivity in three-dimensional networks," *MobiCom*, 2006.
[8] R. P. Bambah, "On lattice coverings by spheres," *Proc. Nat. Sci. India*, no. 10, pp. 25–52, 1954.
[9] E. S. Barnes, "The covering of space by spheres," *Canad. J. Math.*, no. 8, pp. 293–304, 1956.
[10] L. Few, "Covering space by spheres," *Mathematika*, no. 3, pp. 136–139, 1956.
[11] R. P. Bambah, "Lattice coverings with four-dimensional spheres," *Proc. Cambridge Phil. Soc.*, no. 50, pp. 203–208, 1954.
[12] M. N. Bleicher, "Lattice coverings of n-space by spheres," *Canad. J. Math.*, no. 14, pp. 632–650, 1962.
[13] X. Bai, S. Kumar, D. Xuan, Z. Yun, and T. H. Lai, "Deploying wireless sensors to achieve both coverage and connectivity," *ACM Mobihoc*, 2006.
[14] X. Bai, Z. Yun, D. Xuan, T. H. Lai, and W. Jia, "Deploying four-connectivity and full-coverage wireless sensor networks," *IEEE INFOCOM*, 2008.
[15] X. Bai, D. Xuan, Z. Yun, T. H. Lai, and W. Jia, "Complete optimal deployment patterns for full-coverage and k-connectivity (k$\leq$6) wireless sensor networks," *ACM MobiHoc*, 2008.
[16] H. S. M. Coxeter, *Introduction to Geometry*. New York: John Wiley, 1961.
[17] T. C. Hales, "A proof of the kepler conjecture," *Annals of Mathematics*, no. 162, pp. 1065–1185, 2005.
[18] N. Sloane, "The proof of the packing," *Nature*, vol. 425, pp. 126–127, 2003.
[19] G. G. Szpiro, *Kepler's Conjecture:How Some of the Greatest Minds in History Helped Solve One of the Oldest Math Problems in the World*. John Wiley Sons, Inc., 2003.
[20] M. K. Watfa and S. Commuri, "A coverage algorithm in 3d wireless sensor networks," *The 1st International Symposium on Wireless Pervasive Computing*, 2006.
[21] C.-F. Huang, Y.-C. Tseng, and L.-C. Lo, "The coverage problem in three-dimensional wireless sensor networks," *Globalcom*, 2004.
[22] H. Yan, Z. Shi, and J. Cui, "Dbr: Depth-based routing for underwater sensor networks," *IFIP Networking*, 2008.
[23] D. Pompili and T. Melodia, "Three-dimensional routing in underwater acoustic sensor networks," *2nd ACM international workshop on Performance evaluation of wireless ad hoc, sensor, and ubiquitous networks*, 2005.

Basic Lattice	Case A	$\frac{r_c}{r_s} < \frac{2}{\sqrt{3}} : \sigma'_{MIN} = \frac{4\pi r_s^3}{3r_c^3}$;	$\frac{2}{\sqrt{3}} \le \frac{r_c}{r_s} < 2\sqrt{1-\frac{1}{\sqrt{3}}} : \sigma'_{MIN} = \frac{\sqrt{2}\pi(4r_s^2 - r_c^2)r_s^3}{3r_c^3\sqrt{2r_c^2r_s^2 - r_c^4}}$;	$2\sqrt{1-\frac{1}{\sqrt{3}}} \le \frac{r_c}{r_s} : \sigma'_{MIN} = \frac{32\pi(1-\frac{1}{\sqrt{3}})\sqrt{1-\frac{1}{\sqrt{3}}}}{3}$.
	Case B	$\frac{r_c}{r_s} < \frac{4}{\sqrt{5}} : \sigma'_{MIN} = \frac{16\pi r_s^3}{3r_c^2\sqrt{4r_s^2 - r_c^2}}$;	$\frac{r_c}{r_s} \ge \frac{4}{\sqrt{5}} : \sigma'_{MIN} = \frac{5\sqrt{5}\pi}{6}$.	
	Case C	$\frac{r_c}{r_s} < \frac{2}{\sqrt{3}} : \sigma'_{MIN} = \frac{4\pi r_s^3}{3r_c^3}$; $\frac{2}{\sqrt{3}} \le \frac{r_c}{r_s} < 2\sqrt{2}-1 : \sigma'_{MIN} = \frac{2\pi r_s^3(4r_s^2 - r_c^2)}{3r_c^4\sqrt{4r_s^2 - 2r_c^2}}$;	$\sqrt{2}-1 \le \frac{r_c}{r_s} < \frac{4}{\sqrt{5}} : \sigma'_{MIN} = \frac{8\pi r_s^4}{3(4r_c^2r_s^2 - r_c^4)}$;	$\frac{r_c}{r_s} \ge \frac{4}{\sqrt{5}} : \sigma'_{MIN} = \frac{25\pi}{24}$.
	Case D	$\frac{r_c}{r_s} < \sqrt{2} : \sigma'_{MIN} = \frac{4\pi r_s^3}{3r_c^2\sqrt{3r_s^2 - r_c^2}}$;	$\sqrt{2} \le \frac{r_c}{r_s} < \frac{4}{\sqrt{5}} : \sigma'_{MIN} = \frac{8\pi r_s^4}{3(4r_c^2r_s^2 - r_c^4)}$;	$\frac{r_c}{r_s} \ge \frac{4}{\sqrt{5}} : \sigma'_{MIN} = \frac{25\pi}{24}$.
Body Centered Lattice	Case A	$\frac{r_c}{r_s} < \frac{4}{\sqrt{5}} : \sigma'_{MIN} = \frac{8\pi r_s^3}{3r_c^3}$;	$\frac{r_c}{r_s} \ge \frac{4}{\sqrt{5}} : \sigma'_{MIN} = \frac{5\sqrt{5}\pi}{24}$.	
	Case B	$\frac{r_c}{r_s} < \frac{4}{\sqrt{5}} : \sigma'_{MIN} = \frac{16\pi r_s^3}{3r_c^2(2r_c^2 + \sqrt{4r_s^2 - r_c^2})}$;	$\frac{r_c}{r_s} \ge \frac{4}{\sqrt{5}} : \sigma'_{MIN} = \frac{5\sqrt{5}\pi}{6(1+\sqrt{5})}$.	
	Case C	$\frac{r_c}{r_s} < \frac{2\sqrt{3}}{\sqrt{5}} : \sigma'_{MIN} = \frac{\sqrt{3}\pi r_s^3}{r_c^3}$;	$\frac{r_c}{r_s} \ge \frac{2\sqrt{3}}{\sqrt{5}} : \sigma'_{MIN} = \frac{5\sqrt{5}\pi}{24}$.	
	Case D	$\frac{r_c}{r_s} < \frac{4}{\sqrt{5}} : \sigma'_{MIN} = \frac{16\pi r_s^3}{3r_c^3}$;	$\frac{r_c}{r_s} \ge \frac{4}{\sqrt{5}} : \sigma'_{MIN} = \frac{20\sqrt{5}\pi}{3}$.	
	Case E	$\frac{r_c}{r_s} < \frac{4}{\sqrt{5}} : \sigma'_{MIN} = \frac{16\pi r_s^3}{3r_c^2(2r_c^2 + \sqrt{4r_s^2 - r_c^2})}$;	$\frac{r_c}{r_s} \ge \frac{4}{\sqrt{5}} : \sigma'_{MIN} = \frac{5\sqrt{5}\pi}{6(1+\sqrt{5})}$.	
	Case F	$\frac{r_c}{r_s} < \frac{4}{\sqrt{7}} : \sigma'_{MIN} = \frac{16\pi r_s^3}{9r_c^3}$;	$\frac{4}{\sqrt{7}} \le \frac{r_c}{r_s} < \frac{4}{\sqrt{5}} : \sigma'_{MIN} = \frac{32\pi r_s^3}{3r_c(16r_s^2 - r_c^2)}$;	$\frac{r_c}{r_s} \ge \frac{4}{\sqrt{5}} : \sigma'_{MIN} = \frac{5\sqrt{5}\pi}{24}$.
	Case G	$\frac{r_c}{r_s} < \frac{4}{\sqrt{5}} : \sigma'_{MIN} = \frac{16\pi r_s^3}{3r_c^3}$;	$\frac{r_c}{r_s} \ge \frac{4}{\sqrt{5}} : \sigma'_{MIN} = \frac{20\sqrt{5}\pi}{3}$.	
	Case H	$\frac{r_c}{r_s} < \frac{2}{\sqrt{3}} : \sigma'_{MIN} = \frac{16\pi r_s^3}{9r_c^3}$;	$\frac{2}{\sqrt{3}} \le \frac{r_c}{r_s} < \sqrt{2} : \sigma'_{MIN} = \frac{2\pi r_s^2}{3(r_c^2 - r_s^2)}$;	$\frac{r_c}{r_s} \ge \sqrt{2} : \sigma'_{MIN} = \frac{2\pi}{3}$.
Optimal		$\frac{r_c}{r_s} < \frac{9}{\sqrt{43}} : \sigma_{MIN} = \frac{4\pi r_s^3}{3r_c^2\sqrt{3r_s^2 - r_c^2}}$;	$\frac{9}{\sqrt{43}} \le \frac{r_c}{r_s} < \frac{2\sqrt{3}}{\sqrt{5}} : \sigma_{MIN} = \frac{\sqrt{3}\pi r_s^3}{r_c^3}$;	$\frac{r_c}{r_s} \ge \frac{2\sqrt{3}}{5} : \sigma_{MIN} = \frac{5\sqrt{5}\pi}{24}$.

Fig. 7. Comprehensive results of three cases for both basic lattice patterns and body-centered lattice patterns to achieve full coverage and 6-connectivity. σ'_{MIN} denotes the minimum covering density in each case. σ_{MIN} denotes the the minimal covering density among all cases.

[24] W. Cheng, A.Teymorian, L. Ma, X. Cheng, X. Lu, and Z. Lu, "Underwater localization in sparse 3d acoustic sensor networks," *IEEE INFOCOM*, 2008.

[25] Z. Zhou, J. Cui, and A. Bagtzoglou, "Scalable localization with mobility prediction for underwater sensor networks," *IEEE INFOCOM*, 2008.

[26] S. Megerian, F. Koushanfar, G. Qu, G. Veltri, and M. Potkonjak, "Exposure in wireless sensor networks: Theory and practical solutions," *Wireless Networks*, vol. 8, no. 5, pp. 443–454, 2002.

[27] Y. Zhou and K. Charkrabarty, "Sensor deployment and target localization based on virtual force," *Proceedings of IEEE InfoCom*, pp. 1293–1303, 2003.

[28] Q. Cao, T. Yan, J. A. Stankovic, and T. F. Abdelzaher, "Analysis of target detection performance for wireless sensor networks," *International Conference on Distributed Computing in Sensor Networks (DCOSS)*, 2005.

[29] M. Zuniga and B. Krishnamachari, "Analyzing the transitional region in low power wireless links," *Technical Report 04-823, University of Southen California*, 2004.

APPENDIX

We brief the proof for Theorem 2. Following the same methodology in Section V-A, there are two steps in the proof.

In the first step, we summarize all regular patterns with 6-connectivity into a small set of cases that are shown as follows.

– For each lattice point at basic lattice patterns, six connectivity links are:

Case A: Two axle sets.

Case B: Four edges and two side diagonals in a plane going through lateral faces.

Case C: Four edges in a plane going through lateral faces, and two base diagonals.

Case D: Four edges and two base diagonals in a plane going through the base.

– For each lattice point at body-centered lattice patterns, six connectivity links are:

Case A: Two axle sets.

Case B: Four edges and two side diagonals in a plane going through lateral faces.

Case C: Six body diagonals.

Case D: Four edges in a plane going through lateral faces, and two base diagonals.

Case E: Four edges and two base diagonals in a plane going through the base.

Case F: Two edges in a line, and four body diagonals in a plane.

Case G: Two edges in a line along the direction of height, two base diagonals and two body diagonals.

Case H: Two base diagonals, and four body diagonals in a plane.

In the second step, we first obtain the minimal covering density σ'_{MIN} for each case by constructing and then solving nonlinear optimization problems. We present the comprehensive results of all cases in Fig. 7. From the results shown in Fig. 7, we then obtain the minimal covering density σ_{MIN} for each interval of r_c/r_s by comparison. Each σ_{MIN} value is corresponding to a specific V_{MAX} value of the seed parallelepiped, which in turn decides the lattice pattern details. This concludes the proof for Theorem 2.